We are IntechOpen, the world's leading publisher of Open Access books Built by scientists, for scientists

4,800
Open access books available

122,000
International authors and editors

135M
Downloads

Our authors are among the

154
Countries delivered to

TOP 1%
most cited scientists

12.2%
Contributors from top 500 universities

WEB OF SCIENCE™

Selection of our books indexed in the Book Citation Index in Web of Science™ Core Collection (BKCI)

Interested in publishing with us?
Contact book.department@intechopen.com

Numbers displayed above are based on latest data collected.
For more information visit www.intechopen.com

9

Revisions to Code Provisions for Site Effects and Soil-Structure Interaction in Mexico

J. Avilés[1] and L.E. Pérez-Rocha[2]
[1]*Instituto Mexicano de Tecnología del Agua*
[2]*Instituto de Investigaciones Eléctricas*
México

1. Introduction

The seismic hazard in Mexico has been re-evaluated recently and now we can estimate the maximum acceleration on rock for any given site in the country. This is the starting point for constructing site-specific earthquake design spectra that explicitly include the effects of soil dynamic amplification (site effects). The effects of soil-structure interaction (SSI) can be accounted for in two stages: first in the elastic design spectrum, considering the enlargement of the period and the increase in damping; and then in the strength reduction factor, taking into consideration the global ductility reduction.

Site effects refer to the dynamic amplification of ground motion due to the local geotechnical characteristics of the subsoil. These effects are reflected in the seismic design coefficients specified by building codes in terms of site- and structure-response amplification factors. The SSI effects, on the other hand, refer to the modification of the foundation motion with respect to the free-field ground motion due to the flexibility of the supporting soil. In building codes, however, these effects are generally accounted for modifying the dynamic properties (natural period and damping ratio) of the original structure and evaluating the response of the modified structure to the prescribed free-field motion specified by a design spectrum.

A new approach to determine earthquake design spectra including site and SSI effects has been incorporated in the CFE Seismic Design Code (MDOC), a model design code in Mexico (Tena-Colunga et al., 2009). The previous version of the MDOC was published by the Federal Electricity Commission in 1993, so an in-depth review was mandatory in order to update the code for 2008. In the absence of state seismic codes, the MDOC is legally used in the entire nation for earthquake design of different structure types. The MDOC provides expressions to determine earthquake design spectra at any location in the country, which makes unnecessary the use of conventional zoning maps. These spectra, which have realistic shape and size for elastic response, are then reduced by two separate factors to account for the nonlinear structural behavior and overstrength.

2. Site effects

It is well recognized that seismic hazard varies significantly throughout the country and that it cannot be described in detail by means of regional spectra for different types of soil.

Thus, it is necessary to construct site-specific earthquake design spectra, which depend mainly on the proximity from the place to the tectonic sources and on the local subsoil conditions. In the seismic behavior of structures, several response factors associated with the source, the wave's path, the site and the structure itself are involved. In order to simplify the problem, a design earthquake motion at the bedrock is specified by the MDOC, in such a way that the effects of source and wave's path are considered implicitly. In this way, it only remains to account for the site and SSI effects on the structural response. To do this, the simplified reference model shown in fig. 1 is used. This is formed by a modal oscillator placed on a rigid foundation that is embedded into an equivalent stratum with elastic bedrock.

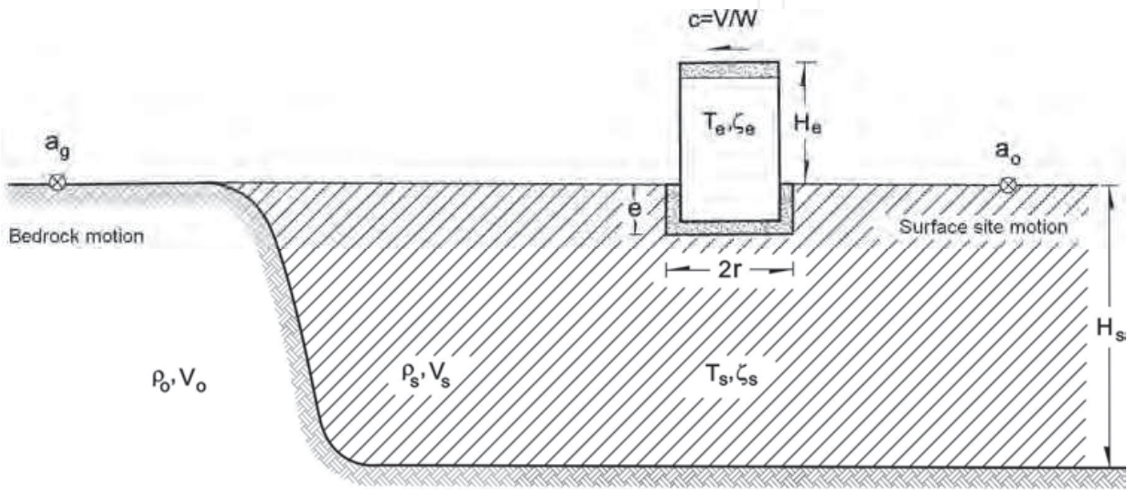

Fig. 1. Simplified reference model to account for site effects and SSI.

For the analyses presented here, a soft soil site (UAPP) located in the city of Puebla with dominant period T_s=1.25 *s*, soil/bedrock impedance ratio $p_s=\rho_s V_s/\rho_o V_o$=0.2, Poisson's ratio ν_s=0.4 and hysteretic damping ratio ζ_s=0.05 has been considered. The value of the site period corresponds to a shear-wave velocity V_s=80 *m/s* and stratum thickness H_s=25 *m*.
Based on the considered model, a new approach to specify earthquake design spectra for arbitrary locations in Mexico has been developed. These spectra realistically represent the levels of strength and displacement demands that would take place in single elastic structures during the design earthquake motion. It is evident that the multi-degree-of-freedom effects in real buildings are not accounted for.

2.1 Acceleration design spectrum

In the MDOC, the seismic hazard was re-evaluated with the use of both deterministic and probabilistic approaches, using spectral attenuation relations developed specifically for the different seismic sources affecting Mexico. The map of fig. 2 shows the nationwide distribution of peak rock acceleration, a_g, for design of standard occupancy structures. This map was produced with a computer program developed for this purpose. The approach proposed to construct elastic design spectra is based on the value of this ground-motion parameter. Next, site- and structure-response factors are developed to account for the peak dynamic amplification of soil and structure responses, respectively. The nonlinear soil

behavior is considered with two additional factors, one for the site period shift and other for the site response reduction, using soil properties (shear modulus and damping ratio) consistent with the shear strain.

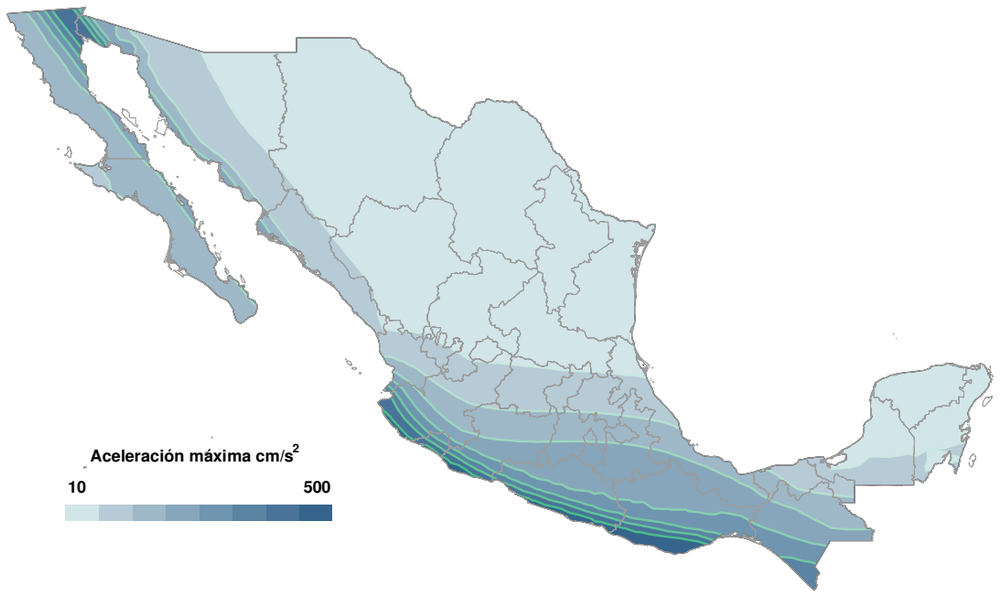

Fig. 2. Distribution of peak rock acceleration in Mexico for design of standard occupancy structures.

With these general ideas in mind, the following steps have to be taken to construct site-specific earthquake design spectra:

1. Compute the distance factor as $F_d=a_g/500$, which is equal to unity near the subduction seismic source. This parameter expresses not only the seismic-wave attenuation with distance, but also the filtering of the high-frequency components of the earthquake excitation.
2. From geotechnical information of the site soil profile, compute the dominant soil period as follows:

$$T_s = 4\sqrt{\left(\sum_{n=1}^{N}\frac{h_n}{G_n}\right)\left(\sum_{n=1}^{N}\rho_n h_n (w_n^2 + w_n w_{n-1} + w_{n-1}^2)\right)} \tag{1}$$

where G_n and ρ_n are the shear modulus and mass density of the nth layer of thickness h_n; $w_o=0$ at the bedrock and

$$w_n = \frac{\sum_{i=1}^{n} h_i/G_i}{\sum_{i=1}^{N} h_i/G_i}; \quad n=1,2,...,N \tag{2}$$

is a static approximation for the fundamental mode of vibration. With T_s known, the effective shear-wave velocity $V_s=4H_s/T_s$ is computed over the depth $H_s=\Sigma h_n$ This novel

procedure is found to give more accurate results than those obtained by using the average shear-wave velocity of the surficial soils, which ignores the layer sequence in the soil profile.

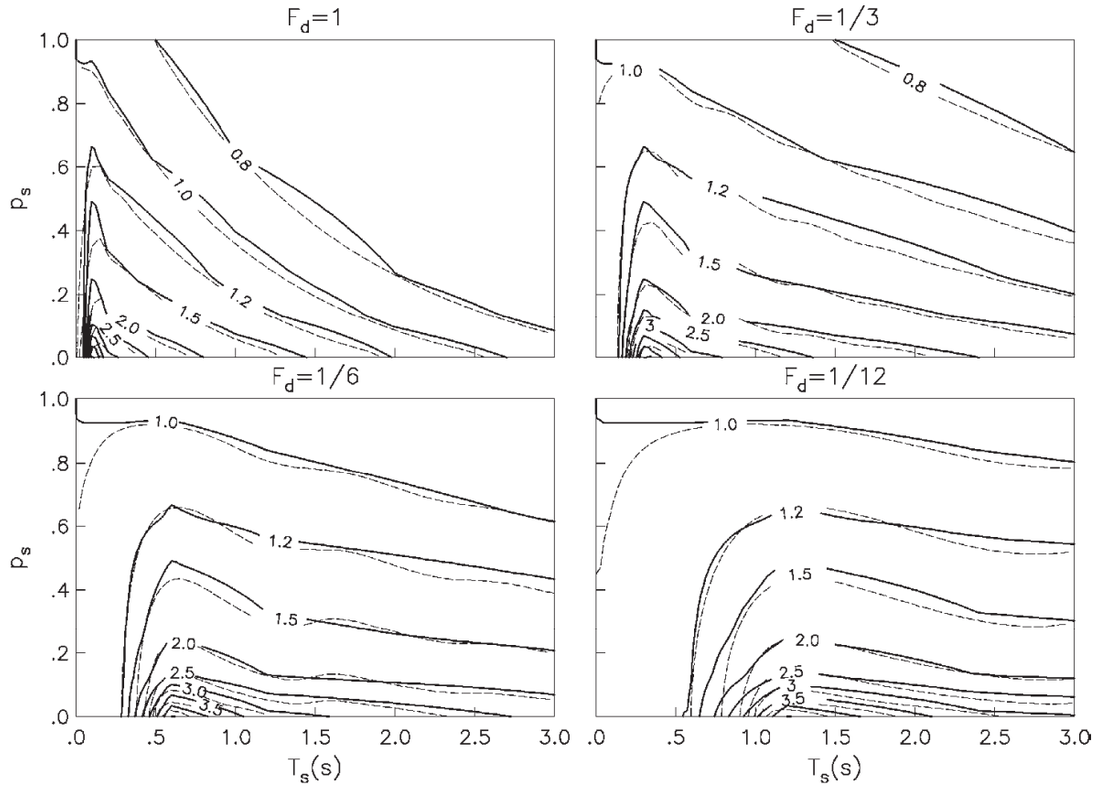

Fig. 3. Contours of F_s derived from site response analysis (dashed line) and by linear interpolation of data in table 1 (solid line).

3. Assuming linear soil behavior, the site-response amplification factor $F_s=a_o/a_g$ is obtained. The values for this factor are based on site response analysis, using the input power spectrum of the rock excitation (Park, 1995) and through application of the random vibration theory (Boore & Joyner, 1984) to predict peak responses. The theoretical results are shown in fig. 3 and the discrete values specified by the MDOC are tabulated in table 1 as a function of $T_s' = T_s\sqrt{F_d}$ and the impedance ratio p_s between soil and bedrock.

T_s' / p_s	0.00	0.05	0.10	0.20	0.50	1.00	2.00	3.00
1.000	1.00	1.00	1.00	1.00	1.00	1.00	1.00	1.00
0.625	1.00	1.08	1.23	1.12	1.00	1.00	1.00	1.00
0.250	1.00	1.18	1.98	1.60	1.40	1.12	1.00	1.00
0.125	1.00	1.20	2.64	2.01	1.69	1.32	1.00	1.00
0.000	1.00	1.22	4.51	3.17	2.38	1.75	1.19	1.00

Table 1. Values of the site amplification factor F_s.

4. Depending on the level of shaking, soil/rock impedance ratio and soil type, the following factors are used to account for the nonlinear soil behavior:

$$F_n^d = \begin{cases} 1-(1-\hat{F}_n^d)\dfrac{T_s}{1.5}, & \text{if } T_s \le 1.5\ s \\ \hat{F}_n^d, & \text{if } T_s > 1.5\ s \end{cases} \tag{3}$$

p_s \ F_d	0.00	0.10	0.20	0.30	0.40	0.50	0.75	1.00
1.000	1.00	0.97	0.93	0.90	0.86	0.83	0.75	0.71
0.625	1.00	0.95	0.91	0.89	0.85	0.82	0.71	0.68
0.250	1.00	0.93	0.87	0.82	0.77	0.73	0.63	0.56
0.125	1.00	0.92	0.84	0.75	0.67	0.64	0.58	0.53
0.000	1.00	0.90	0.78	0.66	0.58	0.54	0.53	0.50

Table 2. Values of the nonlinear factor $\hat{F}_n^d$ for sands and gravels.

p_s \ F_d	0.00	0.10	0.20	0.30	0.40	0.50	0.75	1.00
1.000	1.00	0.98	0.95	0.91	0.87	0.85	0.79	0.75
0.625	1.00	0.97	0.94	0.93	0.90	0.88	0.81	0.79
0.250	1.00	0.96	0.93	0.91	0.87	0.85	0.77	0.74
0.125	1.00	0.93	0.85	0.76	0.70	0.67	0.61	0.56
0.000	1.00	0.82	0.63	0.46	0.36	0.32	0.31	0.28

Table 3. Values of the nonlinear factor $\hat{F}_n^d$ for clays and cohesive soils.

$$F_n^s = \begin{cases} 1-(1-\hat{F}_n^s)\dfrac{T_s}{1.5}, & \text{if } T_s \le 1.5\ s \\ \hat{F}_n^s, & \text{if } T_s > 1.5\ s \end{cases} \tag{4}$$

where the values of $\hat{F}_n^d$ and $\hat{F}_n^s$ are listed in tables 2-3 and 4-5, respectively. While F_n^d expresses the site response reduction due to an increase in damping, $1/F_n^s$ expresses the site period shift due to a decrease in stiffness. Note that these factors tend to unity for very short site period, corresponding to hard rock conditions.

p_s \ F_d	0.00	0.10	0.20	0.30	0.40	0.50	0.75	1.00
1.000	1.00	0.99	0.98	0.97	0.96	0.95	0.95	0.95
0.625	1.00	0.98	0.97	0.93	0.90	0.89	0.89	0.89
0.250	1.00	0.97	0.93	0.86	0.81	0.79	0.79	0.79
0.125	1.00	0.97	0.92	0.85	0.80	0.78	0.78	0.78
0.000	1.00	0.97	0.92	0.85	0.80	0.78	0.78	0.78

Table 4. Values of the nonlinear factor $\hat{F}_n^s$ for sands and gravels.

p_s \ F_d	0.00	0.10	0.20	0.30	0.40	0.50	0.75	1.00
1.000	1.00	1.00	1.00	1.00	1.00	1.00	1.00	1.00
0.625	1.00	1.00	1.00	0.99	0.99	0.99	0.99	0.99
0.250	1.00	0.99	0.98	0.96	0.94	0.93	0.93	0.93
0.125	1.00	0.98	0.95	0.90	0.86	0.84	0.84	0.84
0.000	1.00	0.95	0.88	0.77	0.69	0.67	0.66	0.66

Table 5. Values of the nonlinear factor $\hat{F}_n^s$ for clays and cohesive soils.

5. The peak soil acceleration is obtained from the peak rock acceleration multiplied by the site and nonlinear factors, as follows:

$$a_o = F_n^d F_s a_g \tag{5}$$

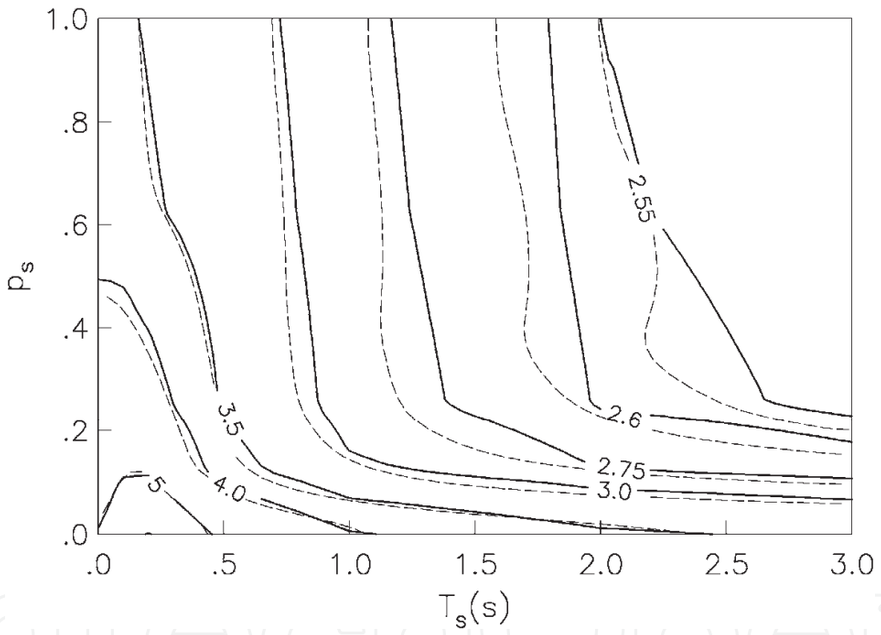

Fig. 4. Contours of F_r derived from site-structure response analyses (dashed line) and by linear interpolation of data in table 6 (solid line).

6. The seismic coefficient that defines the plateau height of the design spectrum is given by

$$c = F_r a_o \tag{6}$$

where F_r is the structure-response amplification factor. The values for this factor are based on the random vibration analysis of a single oscillator subjected to a base excitation passed through the site soil profile. The theoretical results are shown in fig. 4 and the discrete values specified by the MDOC are listed in table 6 as a function of T_s and p_s. As the distance factor has little influence on these results, it has been ignored.

T_s / p_s	0.00	0.05	0.10	0.20	0.50	1.00	2.00	3.00
1.000	2.50	2.50	2.50	2.50	2.50	2.50	2.50	2.50
0.625	2.50	3.80	3.74	3.57	3.26	2.81	2.56	2.51
0.250	2.50	4.36	4.41	4.27	3.45	2.85	2.59	2.53
0.125	2.50	4.74	4.91	4.90	3.70	3.06	2.75	2.65
0.000	2.50	5.27	5.66	6.02	4.81	4.05	3.58	3.40

Table 6. Values of the structural amplification factor F_r.

7. The lower and upper periods of the flat part of the design spectrum are given by

$$T_a = 0.35\frac{T_s}{F_n^s} \geq 0.1\ s \tag{7}$$

$$T_b = 1.2\frac{T_s}{F_n^s} \geq 0.6\ s \tag{8}$$

These expressions are intended to cover not only the peak structural response at the first soil period, but also that at the second one ($\approx T_s/3$). The upper period is taken 20% greater than the site period to account for differences between the computed and actual values of T_s.

8. In terms of the natural vibration period T_e and viscous damping ratio ζ_e, the acceleration design spectrum has the following basic representation:

$$\frac{Sa}{g} = \begin{cases} a_o + (\beta c - a_o)\dfrac{T_e}{T_a}, & \text{if } T_e < T_a \\ \beta c, & \text{if } T_a \leq T_e < T_b \\ \beta c \dfrac{T_b}{T_e}, & \text{if } T_b \leq T_e < T_c \\ \beta c \dfrac{T_b}{T_c} p_c \left(\dfrac{T_c}{T_e}\right)^2, & \text{if } T_e \geq T_c \end{cases} \tag{9}$$

where $p_c = k + (1-k)(T_c/T_e)^2$, with $k = 2.3 - 1.6T_s \geq 0.2$, and

$$T_c = \begin{cases} 2\ s, & \text{if } T_b < 2\ s \\ T_b, & \text{if } T_b \geq 2\ s \end{cases} \tag{10}$$

$$\beta = \begin{cases} \beta_o, & \text{if } T_e < T_c \\ 1 + (\beta_o - 1)\dfrac{T_c}{T_e}, & \text{if } T_e \geq T_c \end{cases} \tag{11}$$

where $\beta_o = (0.05/\zeta_e)^{0.45}$. In the specification of the design spectrum, a nominal damping value of 5% is considered. To account for the supplemental damping due to SSI or mechanical damping devices, the reduction factor β has been introduced. This tends to unity for long-period ordinates, which are independent of the damping value.

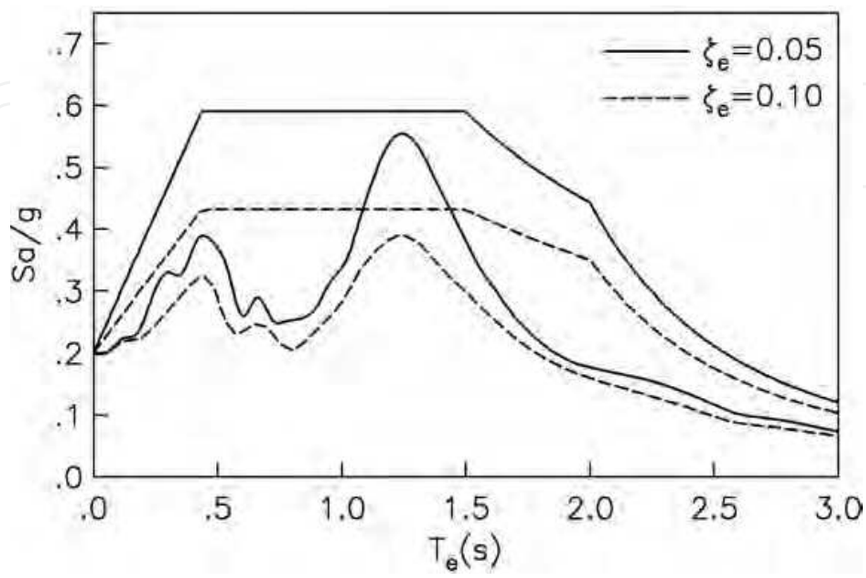

Fig. 5. Acceleration, response and design spectra for site UAPP considering two values of damping.

Following the procedure described above, site-dependent elastic design spectra can be constructed, the shape and size of which are based on the knowledge of peak rock acceleration, site-source distance, dominant soil period and soil/bedrock impedance ratio. For site UAPP, the ensuing spectra for 5 and 10% of damping are shown in fig. 5, along with the corresponding response spectra for the 15 June 1999 Tehuacán earthquake recorded at this site and scaled to the peak rock acceleration specified by the MDOC, without any change in the frequency content and duration characteristics. This normal faulting earthquake of magnitude Mw=7.0 occurred inland 125 *km* from the city of Puebla. Here, it is used as the input control motion at the ground surface.

2.2 Displacement design spectrum

The spectral shapes for $T_e<T_c$ have been in use for many years in Mexican building codes. For $T_e>T_c$, however, a new descending branch is proposed in order to have a better description of the displacement design spectrum *Sd*. Specifically, the limit of this spectrum for very long period must tend to the peak ground displacement D_{max}. In view of the relationship between spectral displacement and acceleration,

$$Sd = \frac{T_e^2}{4\pi^2} Sa \tag{12}$$

this long-period limit can only be achieved if the acceleration design spectrum decays at least as fast as T_e^2. For a slower decay, the displacement design spectrum tends incorrectly to

infinity as the structure period increases. As can be seen in fig. 6, the observed spectral displacements at site UAPP are well represented by the code spectral displacements. It is interesting to note that values of *Sd* larger than D_{max} can occur for natural vibration periods nearby the site period.

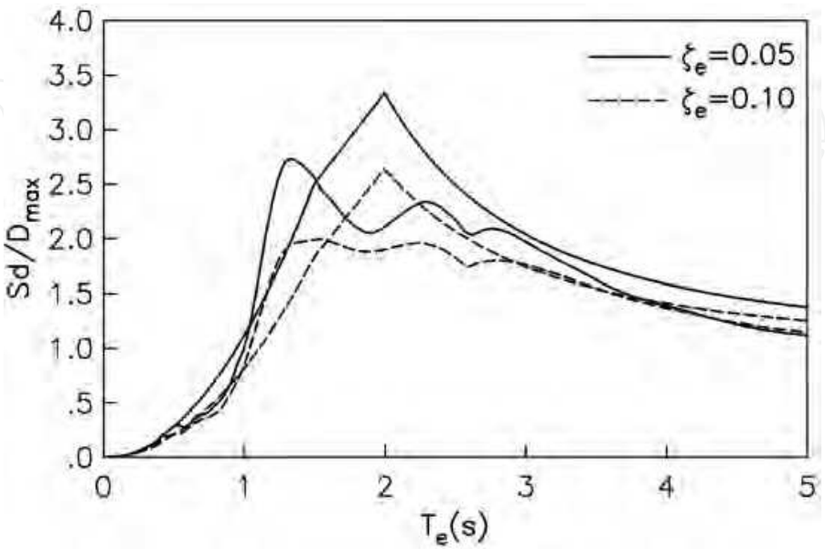

Fig. 6. Displacement, response and design spectra for site UAPP considering two values of damping.

When k<1, the peak spectral displacement occurs at T_e=T_c and is given by

$$Sd_{max} = \frac{g}{4\pi^2}\beta_o c T_b T_c \tag{13}$$

If k≥1, the peak spectral displacement occurs at T_e=∞ and converges to the peak ground displacement given by

$$D_{max} = \frac{g}{4\pi^2} k c T_b T_c \tag{14}$$

From eqns. 13 and 14, it can be found that

$$k = \frac{D_{max}}{Sd_{max}/\beta_o} \tag{15}$$

Notice that parameter k has a physical meaning. It represents the ratio of peak ground displacement to peak spectral displacement for 5% of damping. The code values for this parameter cover a wide variety of site conditions, from hard rock (k=1.5) to very soft soils (k=0.2).

3. Soil-structure interaction

The design approach used in most current codes to take the SSI effects into account has not changed over the years: a replacement oscillator represented by the effective period and

damping of the system. The most extensive efforts in this direction were made by Veletsos (1977) and his coworkers. Indeed, their studies form the basis of the SSI provisions currently in use in the US building codes. Although this approach does not account for the ductile capacity of the structure, it has been implemented in many codes in the world for the convenience of using standard fixed-base spectra in combination with the effective period and damping of the system. Nevertheless, seismic regulations that allow reductions in the design base shear by ductility and SSI separately should be taken with caution. This deficiency has been recognized in the last revision to the SSI procedures in the NEHRP design provisions (Stewart et al., 2003). In the MDOC, the SSI effects are expressed by a shift in the fundamental period T_e, an increase in the damping ratio ζ_e and a reduction in the ductility factor Q_e, as a function of the foundation flexibility H_eT_s/H_sT_e. If a design spectrum is specified for a given site, then the earthquake loads and displacements can be computed by entering with the effective period $\tilde{T}_e$, damping $\tilde{\zeta}_e$ and ductility $\tilde{Q}_e$, just as though the structure were fixed at the base.

3.1 Effective period and damping

For elastic conditions, the system's period and damping are defined as the natural period and damping ratio of a replacement oscillator whose resonant harmonic response is equal to that of the SSI system. Introducing some permissible simplifications, the following expressions can be obtained (Avilés & Pérez-Rocha, 1996):

$$\tilde{T}_e = (T_e^2 + T_h^2 + T_r^2)^{1/2} \tag{16}$$

$$\tilde{\zeta}_e = \zeta_e \frac{T_e^3}{\tilde{T}_e^3} + \frac{\zeta_h}{1+2\zeta_h^2}\frac{T_h^2}{\tilde{T}_e^2} + \frac{\zeta_r}{1+2\zeta_r^2}\frac{T_r^2}{\tilde{T}_e^2} \tag{17}$$

where $T_h = 2\pi(M_e/K_h)^{1/2}$ and $T_r = 2\pi(M_e(H_e+e)^2/K_r)^{1/2}$ are the natural periods associated with the rigid-body translation and rocking of the structure with mass M_e, whereas $\zeta_h = \pi C_h/\tilde{T}_e K_h$ and $\zeta_r = \pi C_r/\tilde{T}_e K_r$ are the damping ratios of the soil for the translational and rocking modes of the foundation. The terms K_h,K_r and C_h,C_r are the frequency-dependent springs and dampers by which the soil is replaced for the two vibration modes of the foundation. The springs account for the stiffness and inertia of the soil, whereas the dampers for the energy dissipation by hysteretic behavior and wave radiation in the soil.

The SSI effects on the period and damping are shown in fig. 7 for high-rise (H_e/r=5) and low-rise (H_e/r=2) structures with embedded foundation (e/r=1) in a soil deposit (H_s/r=5). The system period increases with respect to the fixed-base period as the foundation flexibility increases, especially for the high-rise structure. While the system damping increases for the low-rise structure, it may be smaller than the fixed-base damping for the high-rise structure. The damping reduction due to an increased structural response is particularly important for tall buildings, which are more effectively excited by rocking of the foundation. In the MDOC, the value of $\tilde{\zeta}_e$ cannot be taken less than 0.05, the nominal damping value implicit in the design spectrum.

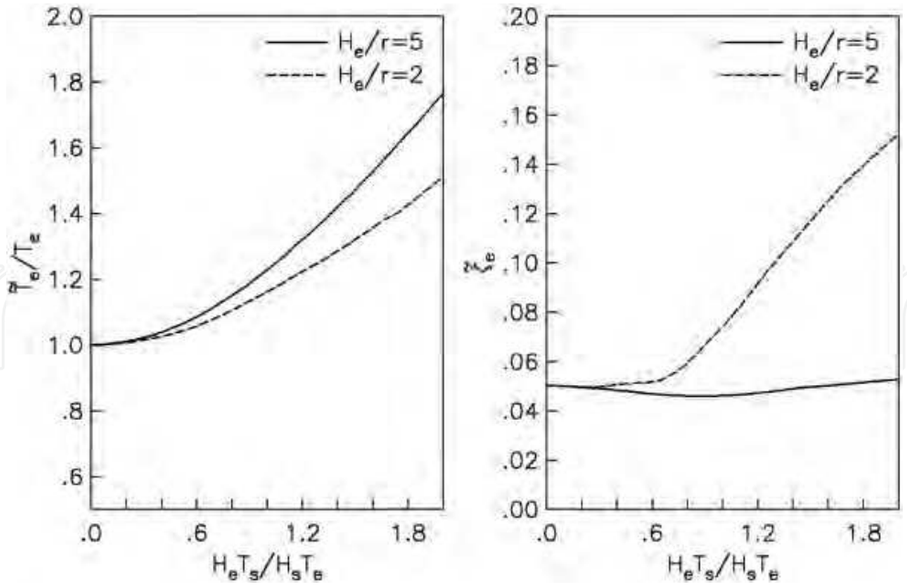

Fig. 7. Effect of SSI on the fundamental period and damping ratio of high- and low-rise structures on flexible foundation.

3.2 Effective ductility

To take the nonlinear structural behavior into account, an equivalent ductility factor is needed to be defined. By equating the maximum plastic deformation of an elastoplastic replacement oscillator with that developed in the SSI system under monotonic loading, the system ductility is found as (Avilés & Pérez-Rocha, 2003)

$$\tilde{Q}_e = 1 + (Q_e - 1)\frac{T_e^2}{\tilde{T}_e^2} \tag{18}$$

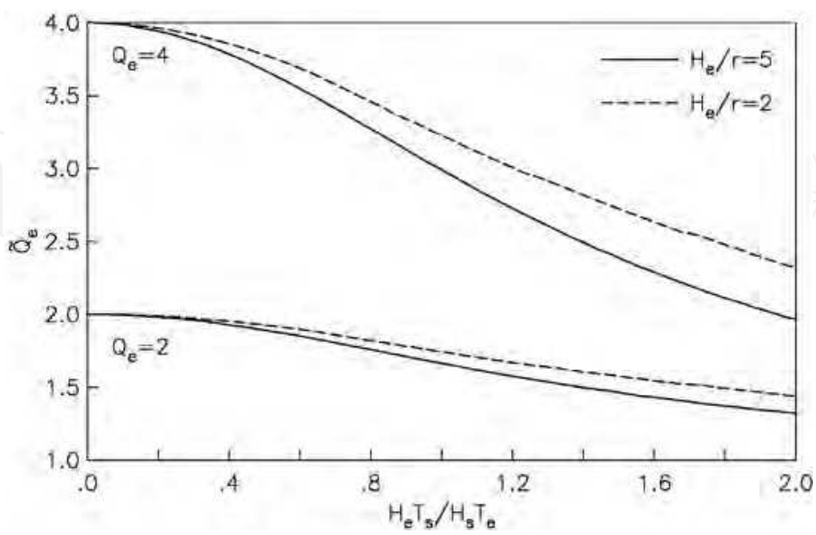

Fig. 8. Effect of SSI on the ductility factor of high- and low-rise structures on flexible foundation.

As shown in fig. 8, the global ductility of the system $\tilde{Q}_e$ reduces with respect to the allowable ductility of the structure Q_e as the foundation flexibility increases. The influence of the structure slenderness is relatively less important. Although the foundation flexibility reduces the ductility factor, the capacity of structural ductility remains unchanged. This apparent paradox stems from the fact that the response of the replacement oscillator includes not only the displacement of the structure itself, but a rigid-body motion of the foundation as well. It is the presence of this motion that reduces the ductility factor.

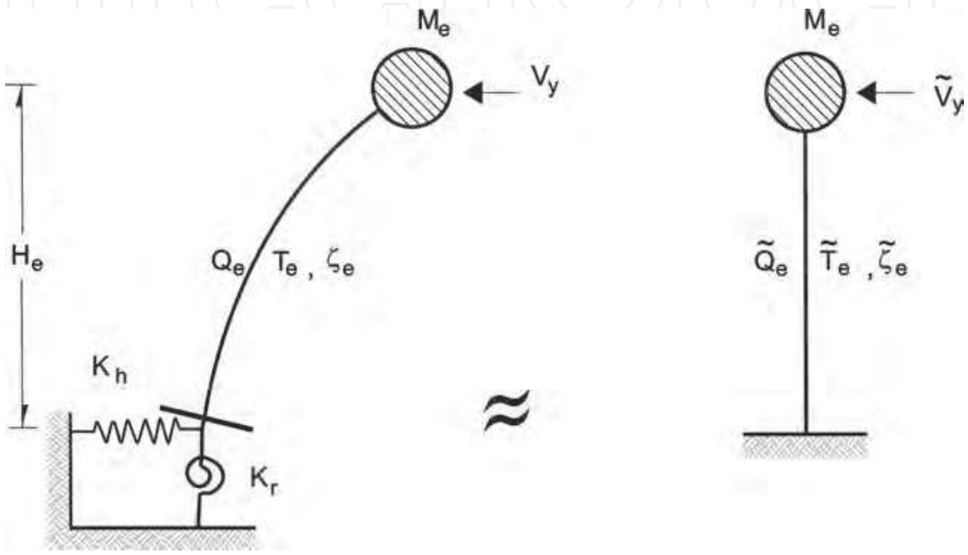

Fig. 9. Analogy between the SSI system and a replacement oscillator.

From the analogy between the SSI system and a replacement oscillator excited by the same base motion, see fig. 9, it is found that their yield resistance and peak displacement are interrelated by

$$V_y = \tilde{V}_y \tag{19}$$

$$Sd = \frac{T_e^2}{\tilde{T}_e^2}\frac{Q_e}{\tilde{Q}_e}\tilde{S}d \tag{20}$$

The difference between the relative inelastic displacement Sd and the total inelastic displacement $\tilde{S}d$ is due to the contribution by the translation and rocking of the foundation. Furthermore, the elastic displacement developed in the replacement oscillator results from the flexibilities of both the structure and foundation.

For a specific case with H_eT_s/H_sT_e=1.33, fig. 10 shows strength spectra obtained with this approach using the input control motion. Base-shear coefficients with ($\tilde{C}_y = \tilde{V}_y / M_e g$) and without ($C_y = V_y / M_e g$) SSI are plotted against the fixed-base period. For Q_e=1, the strength spectrum with SSI shifts toward shorter periods and is a bit less amplified than the strength

spectrum without SSI. For Q_e=4, the resonant peaks associated with the first and second vibration modes of the soil tend to disappear.

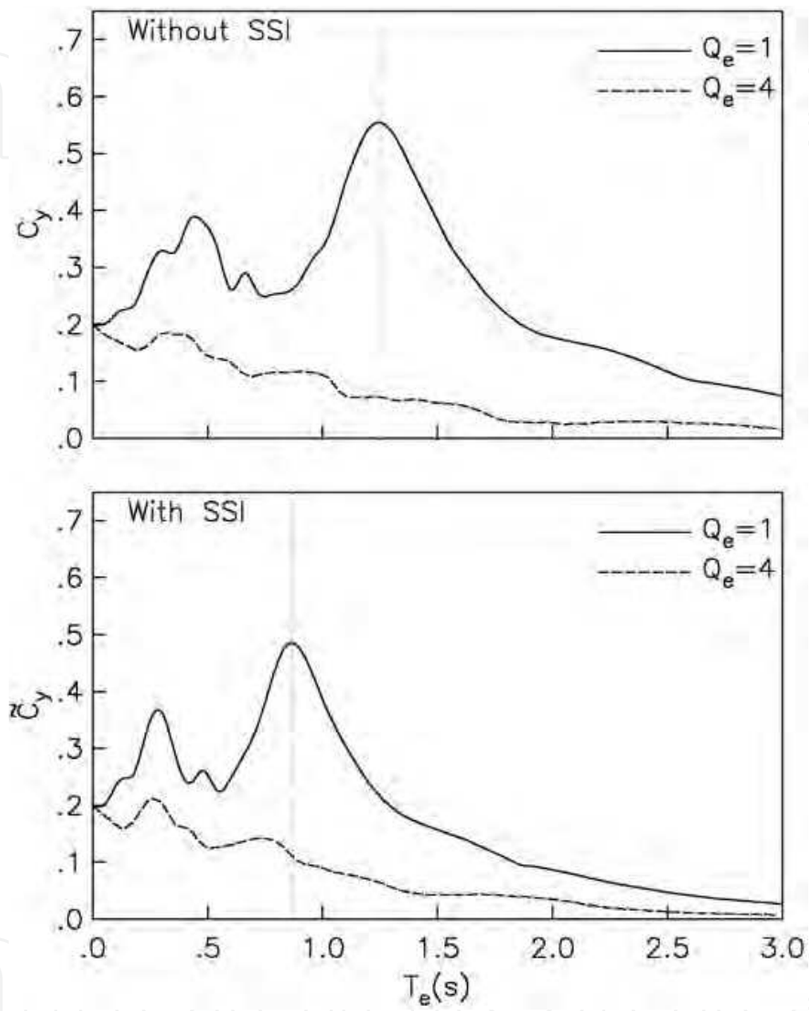

Fig. 10. Strength spectra with and without SSI for elastic and inelastic behavior.

3.3 Strength-reduction factor

For code-designed structures, it is common practice to make use of a strength-reduction factor for estimating inelastic design spectra by reducing elastic design spectra. For a given earthquake, this factor is defined as the ratio between the strength required to have elastic behavior and the strength required for the allowable ductility. The shape of this factor has been extensively studied for the fixed-base condition, using recorded motions and

theoretical considerations. In particular, Ordaz and Pérez-Rocha (1998) observed that it depends on the ratio of the elastic displacement spectrum to the peak ground displacement as follows:

$$Q'_e = 1 + (Q_e - 1)\left(\frac{Sd(T_e,\zeta_e)}{D_{max}}\right)^{1/2} \tag{21}$$

It is apparent that period and damping dependency of Q'_e is implicit in *Sd*. A simplified version of eqn. 21 implemented in the MDOC is the following:

$$Q'_e = \begin{cases} 1 + (Q_e - 1)\sqrt{\dfrac{\beta}{k}}\dfrac{T_e}{T_b}, & \text{if } T_e \le T_b \\ 1 + (Q_e - 1)\sqrt{\dfrac{\beta p_b}{k}}, & \text{if } T_e \ge T_b \end{cases} \tag{22}$$

where $p_b = k + (1-k)(T_b/T_e)^2$. In developing eqn. 22, the following considerations were made: For simplicity, it was decided to have a linear variation between $Q'_e(0) = 1$ and $Q'_e(T_b) = Q'_{max}$, with $Q'_{max} = 1 + (Q_e - 1)\sqrt{Sd_{max}/D_{max}}$ being the maximum value can be reached. The shape of $Q'_e(T_e > T_b)$ results from replacing the corresponding displacement spectrum in eqn. 21. For very long period, β=1 and p_b=k and hence Q'_e tends to Q_e, as dictated by theory.

The fixed-base reduction rule given by eqn. 21 is more general than others reported in the literature, because its period and damping dependence is properly controlled by the actual shape of the elastic displacement spectrum, and not by a smoothed shape obtained empirically. This rule may be readily implemented for flexible-base structures by merely replacing the terms $Q_e - 1$ by $(\tilde{Q}_e - 1)\tilde{T}_e^2/T_e^2$ (from eqn. 18) and *Sd* by $(T_e^2/\tilde{T}_e^2)\tilde{S}d$ (from eqn. 20), with which we have

$$\tilde{Q}'_e = \begin{cases} 1 + (\tilde{Q}_e - 1)\dfrac{\tilde{T}_e}{T_e}\sqrt{\dfrac{\tilde{\beta}}{k}}\dfrac{\tilde{T}_e}{T_b}, & \text{if } \tilde{T}_e \le T_b \\ 1 + (\tilde{Q}_e - 1)\dfrac{\tilde{T}_e}{T_e}\sqrt{\dfrac{\tilde{\beta}\tilde{p}_b}{k}}, & \text{if } \tilde{T}_e \ge T_b \end{cases} \tag{23}$$

The shapes of factors Q'_e and $\tilde{Q}'_e$ are displayed in fig. 11, along with the results given by the equal displacement rule (Veletsos & Newmark, 1960). Contrarily to what happens in many building codes, in this proposal the values of Q'_e can be larger than the ductile capacity Q_e when k<1 corresponding to soft soil sites. This behavior due to site effects is counteracted by SSI. The reason is that SSI tends to shift the structure period to the long-period spectral region, for which the equal displacement rule is applied. Although the representation is not perfect, the proposed reduction rule reproduces satisfactorily the general trends observed for the input control motion.

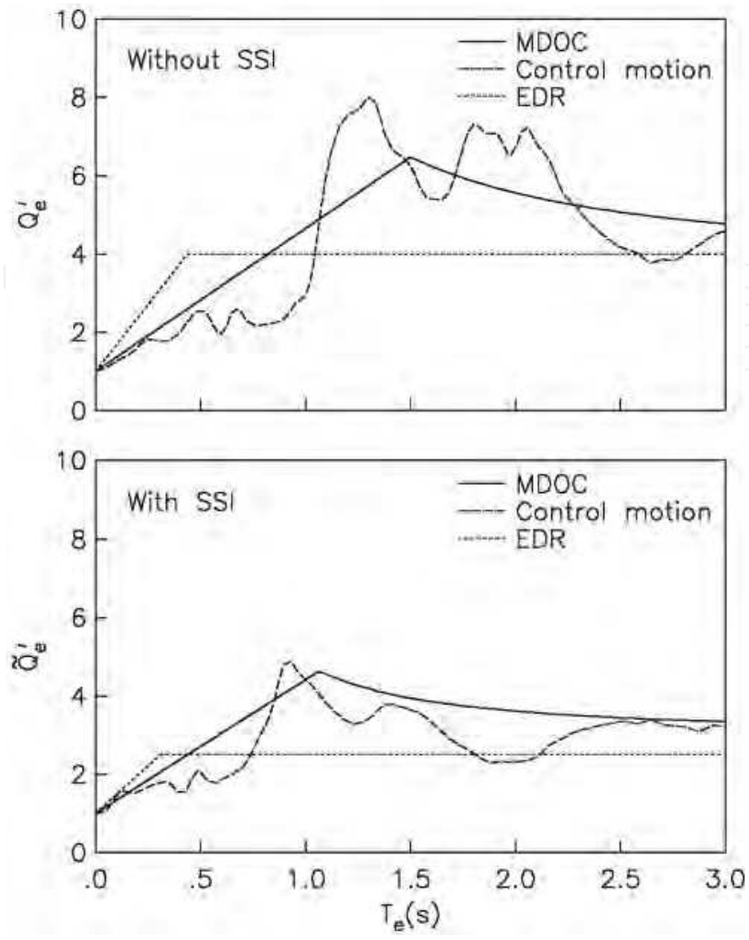

Fig. 11. Strength-reduction factors with and without SSI obtained from code provisions (MDOC and EDR) versus observations.

3.4 Design strength

In view of what has been discussed previously, the required base-shear coefficients with and without SSI can be computed as follows:

$$\tilde{C}_y = \frac{\tilde{S}a(\tilde{T}_e, \tilde{\zeta}_e)/g}{R\tilde{Q}'_e} \tag{24}$$

$$C_y = \frac{Sa(T_e, \zeta_e)/g}{RQ'_e} \tag{25}$$

The elastic acceleration spectra $\tilde{S}a$ and Sa are used to emphasize the fact that the former should be evaluated for $\tilde{T}_e$ and $\tilde{\zeta}_e$, and the latter for T_e and ζ_e. Notice that the overstrength reduction factor R is independent of SSI. Strength design spectra with and without SSI are exhibited in fig. 12, along with strength response spectra for the input control motion. It is clear that the latter spectra are safely covered by the former in the whole period range. Nevertheless, the conservatism inherent in smoothed design spectra overshadows some

important changes by SSI, as those happening in the spectral region between the first and second soil periods.

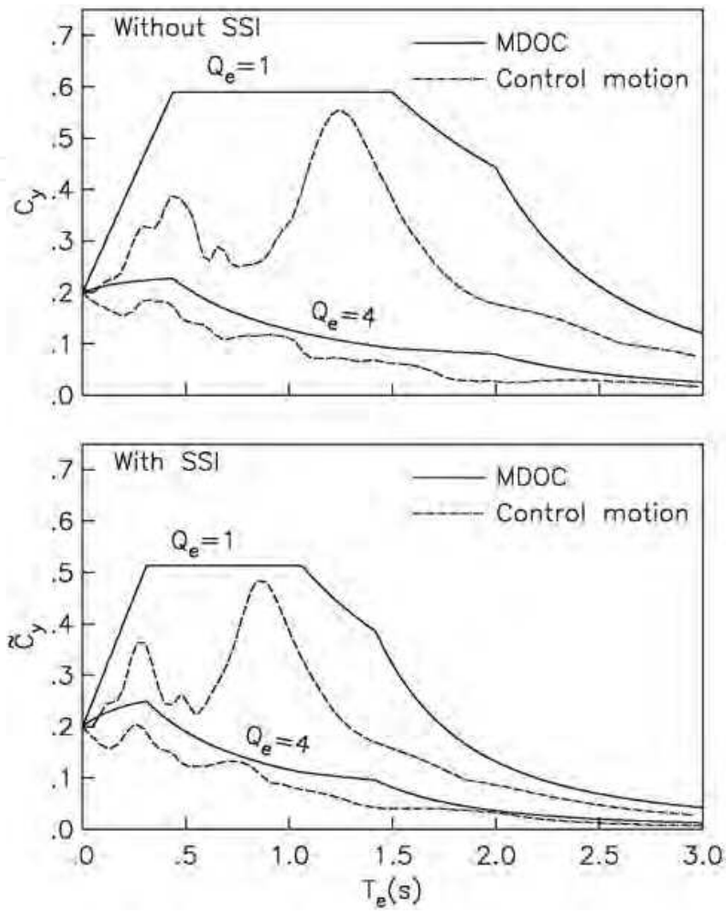

Fig. 12. Design and response strength spectra with and without SSI for elastic and inelastic behavior.

The use of the recommended SSI provisions will increase or decrease the design earthquake forces with respect to the fixed-base values, depending on the dynamic properties of the structure and soil and the characteristics of the earthquake excitation. The lateral displacements will undergo additional changes due to the contribution by the translation and rocking of the foundation. This latter motion may be particularly significant for tall buildings.

A convenient factor to account for modifications of the structural response due to SSI is given by the ratio $\tilde{V}_y / V_y = \tilde{C}_y / C_y$. The results shown in fig. 13 for this SSI factor, derived from the strength design spectra of fig. 12, illustrate the following points: The increments in the base shear are less important than the reductions. While the greater increments arise in nonlinear systems (Q_e=4), the greater reductions arise in linear systems (Q_e=1). The SSI factor can be used to modify the response quantities computed for the structure assumed to be fixed at the base. In the MDOC, the value of $\tilde{V}_y / V_y$ cannot be taken less than 0.7, nor greater than 1.2. It is seen, however, that the calculated reduction can be considerably larger than 30%.

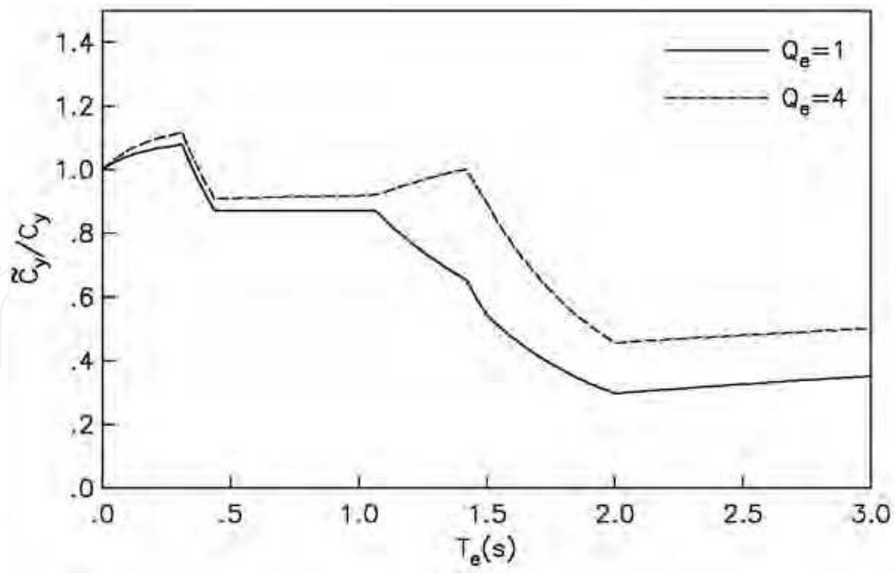

Fig. 13. Variation of the SSI factor for elastic and inelastic behavior.

Finally, the maximum displacement of the flexible-base structure relative to the ground can be determined as

$$\tilde{\delta}_{max} = \frac{\tilde{V}_y}{V_y}\left(\delta_{max} + \frac{V_y}{K_h} + (H_e + e)^2 \frac{V_y}{K_r} \right) \tag{26}$$

where $\delta_{max} = (V_y / K_e) Q_e$ is the maximum displacement of the fixed-base structure, with K_e being the lateral structural stiffness.

4. Conclusions

The site effects and SSI provisions described in this work have been incorporated in the 2008 MDOC seismic design code used in Mexico. A simplified model of the soil and structure that forms the basis of current design practice was investigated. A new approach for constructing site-specific earthquake design spectra was devised, which reflects some research advances made on site response and SSI. The approach is based on the peak rock acceleration determined with a computer program developed for this purpose. Improved site- and structure-response factors to account for the peak dynamic amplification of soil and structure responses were developed. The nonlinear soil behavior was considered with two additional factors, one for the site period shift and other for the site response reduction. These factors should be computed using soil properties consistent with the shear strain. To account for the nonlinear structural behavior, a known site-dependent strength reduction factor properly adjusted to include SSI was implemented. The SSI effects were expressed by a shift in the fundamental period and an increase in the damping ratio for the elastic condition, as well as a reduction in the nominal ductility factor. It was shown that the independent reduction of the design base shear by ductility and SSI is unsuitable, especially for very ductile structures. It is expected that with these improvements to code provisions, the earthquake response of code-designed structures will be assessed more accurately.

5. References

Avilés, J. & Pérez-Rocha, L.E. (1996). Evaluation of Interaction Effects on the System Period and the System Damping due to Foundation Embedment and Layer Depth. *Soil Dynamics and Earthquake Engineering*, Vol. 15, No. 1, pp. 11-27, ISSN 0267-7261

Avilés, J. & Pérez-Rocha, L.E. (2003). Soil-Structure Interaction in Yielding Systems. *Earthquake Engineering and Structural Dynamics*, Vol. 32, No. 11, pp. 1749-1771, ISSN 0098-8847

Avilés, J. & Pérez-Rocha, L.E. (2005). Design Concepts for Yielding Structures on Flexible Foundation. *Engineering Structures*, Vol. 27, No. 3, pp. 443-454, ISSN 0141-0296

Boore, D.M. & Joyner, W.B. (1984). A Note on the Use of Random Vibration Theory to Predict Peak Amplitudes of Transient Signals. *Bulletin of the Seismological Society of America*, Vol. 74, No. 5, pp. 2035-2039, ISSN 0037-1106

Ordaz, M. & Pérez-Rocha, L.E. (1998). Estimation of Strength-Reduction Factors for Elastoplastic Systems: A New Approach. *Earthquake Engineering and Structural Dynamics*, Vol. 27, No. 9, pp. 889-901, ISSN 0098-8847

Park, Y.J. (1995). New Conversion Method from Response Spectrum to PSD Functions. *Journal of Engineering Mechanics*, Vol. 121, No. 12, pp. 1391-1392, ISSN 0733-9399

Stewart, J.P.; Kim, S.; Bielak, J.; Dobry, R. & Power, M.S. (2003). Revisions to Soil-Structure Interaction Procedures in NEHRP Design Provisions. *Earthquake Spectra*, Vol. 19, No. 3, pp. 677-696, ISSN 8755-2930

Tena-Colunga, A.; Mena-Hernández, U.; Pérez-Rocha, L.E.; Avilés, J.; Ordaz, M. & Vilar, J.I. (2009). Updated Seismic Design Guidelines for Model Building Code of Mexico. *Earthquake Spectra*, Vol. 25, No. 4, pp. 869-898, ISSN 8755-2930

Veletsos, A.S. & Newmark, N.M. (1960). Effect of Inelastic Behavior on the Response of Simple Systems to Earthquake Motions. *Proceedings of the 2nd World Conference on Earthquake Engineering*, Tokyo and Kyoto, Japan

Veletsos, A.S. (1977). Dynamics of Structure-Foundation Systems, In: *Structural and Geotechnical Mechanics*, W.J. Hall, (Ed.), pp. 333-361, Prentice-Hall, Englewood Cliffs, USA

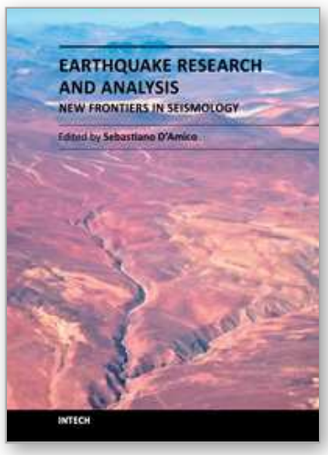

Earthquake Research and Analysis - New Frontiers in Seismology
Edited by Dr Sebastiano D'Amico

ISBN 978-953-307-840-3
Hard cover, 380 pages
Publisher InTech
Published online 27, January, 2012
Published in print edition January, 2012

The study of earthquakes combines science, technology and expertise in infrastructure and engineering in an effort to minimize human and material losses when their occurrence is inevitable. This book is devoted to various aspects of earthquake research and analysis, from theoretical advances to practical applications. Different sections are dedicated to ground motion studies and seismic site characterization, with regard to mitigation of the risk from earthquake and ensuring the safety of the buildings under earthquake loading. The ultimate goal of the book is to encourage discussions and future research to improve hazard assessments, dissemination of earthquake engineering data and, ultimately, the seismic provisions of building codes.

InTech Europe
University Campus STeP Ri
Slavka Krautzeka 83/A
51000 Rijeka, Croatia
Phone: +385 (51) 770 447
Fax: +385 (51) 686 166
www.intechopen.com

InTech China
Unit 405, Office Block, Hotel Equatorial Shanghai
No.65, Yan An Road (West), Shanghai, 200040, China
中国上海市延安西路65号上海国际贵都大饭店办公楼405单元
Phone: +86-21-62489820
Fax: +86-21-62489821

IntechOpen